

*International Conference on magnetic fields in O, B and A stars
 ASP Conference Series, Vol. No.216, 2003
 L.A. Balona, H. Henrichs & T. Medupe, eds.*

The Effects of Magnetic Fields on Line-Driven Hot-Star Winds

Asif ud-Doula

*Department of Physics, North Carolina State University, Raleigh, NC
 27695-8202, USA*

Stanley Owocki

*Bartol Research Institute, University of Delaware, Newark, DE 19716,
 USA*

Abstract. This talk summarizes results from recent MHD simulations of the role of a dipole magnetic field in inducing large-scale structure in the line-driven stellar winds of hot, luminous stars. Unlike previous fixed-field analyses, the MHD simulations here take full account of the dynamical competition between the field and the flow. A key result is that the overall degree to which the wind is influenced by the field depends largely on a single, dimensionless ‘wind magnetic confinement parameter’, η_* ($= B_{eq}^2 R_*^2 / M v_\infty$), which characterizes the ratio between magnetic field energy density and kinetic energy density of the wind. For weak confinement, $\eta_* \leq 1$, the field is fully opened by wind outflow, but nonetheless, for confinement as small as $\eta_* = 1/10$ it can have significant back-influence in enhancing the density and reducing the flow speed near the magnetic equator. For stronger confinement, $\eta_* > 1$, the magnetic field remains closed over limited range of latitude and height above the equatorial surface, but eventually is opened into nearly radial configuration at large radii. Within the closed loops, the flow is channeled toward loop tops into shock collisions that are strong enough to produce hard X-rays. Within the open field region, the equatorial channeling leads to oblique shocks that are again strong enough to produce X-rays and also lead to a thin, dense, slowly outflowing “disk” at the magnetic equator.

1. Introduction

There is extensive evidence that hot-star winds are not the steady, smooth outflows envisioned in the spherically symmetric, time-independent models of Castor, Abbott, and Klein (1975; hereafter CAK), but instead have extensive structure and variability on a range of spatial and temporal scales. Relatively small-scale, stochastic structure – e.g. as evidenced by often quite constant soft X-ray emission (Long & White 1980), or by UV lines with extended black troughs understood to be a signature of a nonmonotonic velocity field (Lucy 1982) – seems most likely a natural result of the strong, intrinsic instability of the line-driving mechanism itself (Owocki 1994; Feldmeier 1995). But larger-scale structure – e.g. as evidence by explicit UV line profile variability in even

low signal-to-noise IUE spectra (Kaper et al. 1996; Howarth & Smith 1995) – seems instead likely to be the consequence of wind perturbation by processes occurring in the underlying star. For example, the photospheric spectra of many hot stars show evidence of radial and/or non-radial pulsation, and in a few cases there is evidence linking this with observed variability in UV wind lines (Telting, Aerts, & Mathias 1997; Mathias et al. 2001).

An alternate scenario – one explored through dynamical simulations in this talk – is that, in at least some hot stars, surface magnetic fields could perturb, and perhaps even channel, the wind outflow, leading to rotational modulation of wind structure that is diagnosed in UV line profiles, and perhaps even to magnetically confined wind-shocks with velocities sufficient to produce the relatively hard X-ray emission seen in some hot-stars. The recent report by Donati et al (2001) of a ca. 1000 G dipole field in θ^1 Ori C suggests that, despite the lack of strong convection zones, hot stars can indeed have magnetic fields.

The focus of the present paper is to carry out MHD simulations of how such magnetic fields on the surface of hot stars can influence their radiatively-driven wind. Our approach here represents a natural extension of the previous studies by Babel & Montmerle (1997a,b; hereafter BM97a,b), which effectively *prescribed* a fixed magnetic field geometry to channel the wind outflow. For large magnetic loops, wind material from opposite footpoints is accelerated to a substantial fraction of the wind terminal speed (i.e. ~ 1000 km/s) before the channeling toward the loop tops forces a collision with very strong shocks, thereby heating the gas to temperatures ($10^7 - 10^8$ K) that are high enough to emit hard (few keV) X-rays. This ‘magnetically confined wind shock’ (MCWS) model was initially used to explain X-ray emission from the Ap-Bp star IQ Aur (BM97a), which has a quite strong magnetic field (~ 4 kG) and a rather weak wind (mass loss rate $\sim 10^{-10} M_\odot/\text{yr}$), and thus can indeed be reasonably modeled within the framework of prescribed magnetic field geometry.

Later, BM97b applied this model to explain the periodic variation of X-ray emission of the O7 star θ^1 Ori C, which has a much lower magnetic field ($\lesssim 1000$ G) and significantly stronger wind (mass loss rate $\sim 10^{-7} M_\odot/\text{yr}$), raising now the possibility that the wind itself could influence the field geometry in a way that is not considered in the simpler fixed-field approach.

The simulation models here are based on an isothermal approximation of the complex energy balance, and so can provide only a rough estimate of the level of shock heating and X-ray generation. But a key advantage over previous approaches is that these models do allow for such a fully dynamical competition between the field and flow. A central result is that the overall effectiveness of magnetic field in channeling the wind outflow can be well characterized in terms of single ‘wind magnetic confinement parameter’ η_* , defined below (§2). In §3 we discuss the key results of our simulations, and in §4 we summarize our main conclusions.

2. The Wind Magnetic Confinement Parameter

As detailed in ud-Doula and Owocki (2002), the relative effectiveness of magnetic fields in confining and/or channeling a wind outflow depends largely on the ratio

of energy densities in the field vs. flow

$$\begin{aligned}\eta(r, \theta) &\equiv \frac{B^2/8\pi}{\rho v^2/2} \approx \frac{B^2 r^2}{\dot{M} v} \\ &= \left[\frac{B_*^2(\theta) R_*^2}{\dot{M} v_\infty} \right] \left[\frac{(r/R_*)^{2-2q}}{1 - R_*/r} \right].\end{aligned}\quad (1)$$

The latter approximations assume a separation in terms of the latitudinal variation of the surface field, $B_*(\theta)$ (e.g. for dipole $B_*^2(\theta) = B_o^2(\cos^2 \theta + \sin^2 \theta/4)$) and radial variation $B(r) = B_*(R_*/r)^q$, with, e.g., for a simple dipole $q = 3$. The right square bracket in eqn (1) represents the spatial variations of this energy ratio and the left square bracket represents a dimensionless constant that characterizes the overall relative strength of field vs. wind. Evaluating this at the magnetic equator ($\theta = 90^\circ$), where the radial wind outflow is in most direct competition with a horizontal orientation of the field; we can thus define an equatorial ‘wind magnetic confinement parameter’,

$$\eta_* \equiv \frac{B_*^2(90^\circ) R_*^2}{\dot{M} v_\infty} = 0.4 \frac{B_{100}^2 R_{12}^2}{\dot{M}_{-6} v_8}. \quad (2)$$

where $\dot{M}_{-6} \equiv \dot{M}/(10^{-6} M_\odot/\text{yr})$, $B_{100} \equiv B_o/(100 \text{ G})$, $R_{12} \equiv R_*/(10^{12} \text{ cm})$, and $v_8 \equiv v_\infty/(10^8 \text{ cm/s})$. For a typical OB supergiant, e.g. ζ Pup, this suggests that significant magnetic confinement or channeling of the wind should require fields of order $\sim 100 \text{ G}$. By contrast, in the case of the sun, with the much weaker mass loss ($\dot{M}_\odot \sim 10^{-14} M_\odot/\text{yr}$) global field $B_o \sim 1 \text{ G}$ is sufficient to yield $\eta_* \simeq 40$, implying a substantial magnetic confinement of the solar coronal expansion. This is consistent with the observed large extent of magnetic loops in optical, UV and X-ray images of the solar corona.

3. Results

We study the dynamical competition between field and wind by evolving our MHD simulations from an initial condition at time $t = 0$, when a dipole magnetic field is suddenly introduced into a previously relaxed, 1D spherically symmetric CAK wind for various assumed values of the wind magnetic confinement parameter η_* . We first confirm that, for sufficiently weak confinement, i.e., $\eta_* \leq 0.01$, the wind is essentially unaffected by the magnetic field. But for models within the range $1/10 < \eta_* < 10$, the field has a significant influence on the wind. For our main parameter study, the variations in η_* are implemented solely through variations in the assumed magnetic field strength, with the stellar and wind parameters fixed at values appropriate to a typical OB supergiant, e.g. ζ Pup. Detailed analysis and results of all these models are presented in ud-Doula and Owocki (2002), here we merely summarize them.

3.1. Global Wind Structure for Strong, Moderate, and Weak Fields

As an example, Figure 1 illustrates the global configurations of magnetic field, density, and radial and latitudinal components of velocity at the final time snapshot, $t = 450 \text{ ksec}$ after initial introduction of the dipole magnetic field. The

top, middle, and bottom rows show respectively results for a weak, moderate, and strong field, characterized by confinement parameters of $\eta_* = 1/10$, 1, and 10.

For the weak magnetic case $\eta_* = 1/10$, the flow effectively extends the field to almost a purely radial configuration everywhere. Nonetheless, the field still has a noticeable influence, deflecting the flow slightly toward the magnetic equator (with peak latitudinal speed $\max(v_\theta) \simeq 70$ km/s) and thereby leading to an increased density and a decreased radial flow speed in the equatorial region. With the increase of η_* , this equatorward deflection becomes more pronounced, with a faster latitudinal velocity component ($\max(v_\theta) \simeq 300$ km/s for $\eta_* = 1$, and > 500 km/s for $\eta_* = 10$), and a correspondingly stronger equatorial change in density and radial flow speed leading to a quite narrow equatorial “disk” of dense, slow outflow. For the strong magnetic case $\eta_* = 10$, the near-surface fields now have a closed-loop configuration out to a substantial fraction of a stellar radius above the surface, but outside and well above the closed region, the flow is quasi-steady.

3.2. Variability of Near-Surface Equatorial Flow

In contrast to this relatively steady, smooth nature of the outer wind, the flow near the star can be quite structured and variable in the equatorial regions. Figure 2 zooms in on the near-star equatorial region, comparing density (upper row, contours), mass flux (arrows), and field lines (lower row) at an arbitrary time snapshot long after the initial condition ($t > 400$ ksec), for three models with magnetic confinement numbers $\eta_* = 1, \sqrt{10}$, and 10.

For all three cases, high-density knots appear at few tenths of R_* above the equatorial surface. These knots are too dense for the the radiative-driving to maintain a net outward acceleration against the inward pull of the stellar gravity. As such, they eventually fall back onto the stellar surface. Although strong magnetic tension can support these knots for a while, it eventually forces them to slide to north or south hemispheres. The animations of the time evolution for these models show that such infalls occur at semi-regular intervals of about 200 ksec.

4. Conclusion

Observational implications of these MHD simulations are discussed in ud-Doula and Owocki (2002). Here, we merely highlight some of our conclusions.

We found that the general effect of magnetic field in channeling the stellar wind depends on the overall ratio of magnetic to flow-kinetic-energy density, as characterized by the wind magnetic confinement parameter, η_* , defined here in eqn. (2). For moderately small confinement, $\eta_* = 1/10$, the wind extends the surface magnetic field into an open, nearly radial configuration. But even at this level, the field still has a noticeable global influence on the wind, enhancing the density and decreasing the flow speed near the magnetic equator. For intermediate confinement, $\eta_* = 1$, the fields are still opened by the wind outflow, but near the surface retain a significant non-radial tilt, channeling the flow toward the magnetic equator with a latitudinal velocity component as high as 300 km/s. On the other hand, for strong confinement, $\eta_* = 10$, the field remains

closed in loops near the equatorial surface. Wind outflows accelerated upward from opposite polarity footpoints are channeled near the loop tops into strong collision, with characteristic shock velocity jumps of up to about 1000 km/s, strong enough to lead to hard (> 1 keV) X-ray emission.

In contrast to previous steady-state, fixed-field models (e.g. BM97a), the time-dependent dynamical models here indicate that stellar gravity pulls the compressed, stagnated material within closed loops into an infall back onto the stellar surface, often through quite complex, intrinsically variable flows that follow magnetic channels randomly toward either the north or south loop footpoint.

Acknowledgements. This research was supported in part by NASA grant NAG5-3530 and NSF grant AST-0097983 to the Bartol Research Institute at the University of Delaware. A. ud-Doula acknowledges support of NASA's Space Grant College program at the University of Delaware.

References

Babel, J. & Montmerle, T. 1997, A&A, 323, 121
 Babel, J. & Montmerle, T. 1997, ApJ, 485, L29
 Castor, J. I., Abbott, D. C., & Klein, R. I. 1975, ApJ, 195, 157
 Donati, J.-F., Wade, G. A., Babel, J., Henrichs, H. F., de Jong, J. A., Harries, T. J. 2001, MNRAS, 326, 1265
 Feldmeier, A. 1995, A&A, 299, 523
 Howarth, I. D. & Smith, K. C. 1995, ApJ, 439, 431
 Kaper, L., Henrichs, H. F., Nichols, J. S., Snoek, L. C., Volten, H., & Zwarthoed, G. A. A. 1996, A&AS, 116, 257
 Long, K. S. & White, R. L. 1980, ApJ, 239, L65
 Lucy, L. B. 1982, ApJ, 255, 286
 Mathias, P., Aerts, C., Briquet, M., De Cat, P., Cuypers, J., Van Winckel, H., Flanders., & Le Contel, J. M. 2001, A&A, 379, 905
 Owocki, S. P., Cranmer, S. R., & Blondin, J. M. 1994, ApJ, 424, 887
 Telting, J. H., Aerts, C., & Mathias, P. 1997, A&A, 322, 493
 ud-Doula, A. & Owocki, S. 2002, ApJ, 576, 413

Discussion

Brown: Am I right in thinking you have no rotation in the results you showed, which could prevent fall back? Also, your results are $\dot{M} = 10^{-6} M_{\odot}/yr$ which is much larger than for Be star winds ($\sim 10^{-9} M_{\odot}/yr$), so, it is not surprising that even very large fields have limited effect.

ud-Doula: Yes, you are right. I did not include rotation in the models I presented here. But I did do a parameter study that included rotation, and those models will be presented by Stan Owocki later in the day.

One important point I wanted to make in this talk is that the mass loss rate alone doesn't determine if magnetic fields can play an important role or not, it is the combination of parameters that define η_* that determines the importance of the field. In general, low mass loss rate implies high value of η_* even for moderate field strengths (10-100 G), and this is particularly true for Be stars. So modest magnetic fields could play a significant role in Be stars.

Wade: You made the point that your models predict a disc around $\theta^1 Ori C$ that is highly variable. However, the optical spectroscopic diagnostics that probe the disk (in particular, the $H\alpha$ and $H\beta$ and He 4686 emission lines) show that it is stable over many, many rotations. This seems to be telling us that the disk is quite stable. Can you reconcile these results?

ud-Doula: The variability I am suggesting is mostly confined to region near the surface of the star, the flow far away from the surface, including the disk, may be quasi-steady.

Steinitz: Your MHD equations did not include an essential mechanism: the DME (Diamagnetic Effect). Inclusion may change your fitting parameters drastically since it is not clear that exclusion of DME describes anything close to real physics.

ud-Doula: Indeed I have not included DME explicitly in my MHD equations. As such, I do not know how much DME can influence my results, but this is something I should, perhaps, look into in the near future.

Ignace: I know that your models do not include shock generation in the wind at large distances, but do you think that the hot gas in the equatorial region from the magnetically-guided self-colliding wind will dominate the X-ray emission?

ud-Doula: I think you are right, it will dominate the hard X-ray emission. As for the soft X-ray, likely the result of the strong instabilities in the wind, can be formed at large distances.

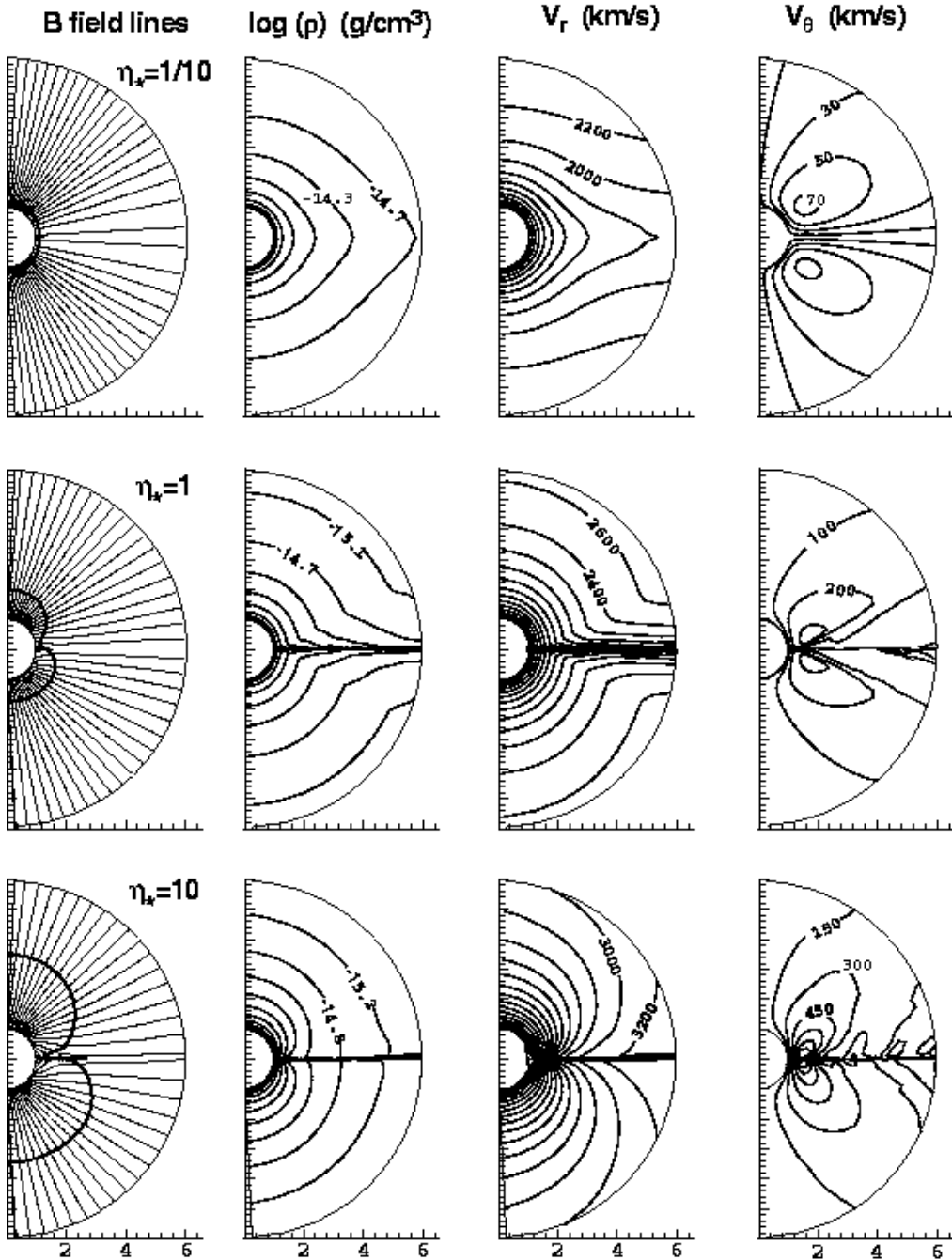


Figure 1. Comparison of overall properties at the final simulation time ($t = 450$ sec) for 3 MHD models, chosen to span a range of magnetic confinement from small (top row; $\eta_* = 1/10$), to medium (middle row; $\eta_* = 1$), to large (bottom row; $\eta_* = 10$). The leftmost panels show magnetic field lines, together with the location (bold contour) of the Alfvén radius, where the radial flow speed equals the Alfvén speed. From left to right, the remaining columns show contours of $\log(\rho)$, V_r (km/s), and V_θ (km/s).

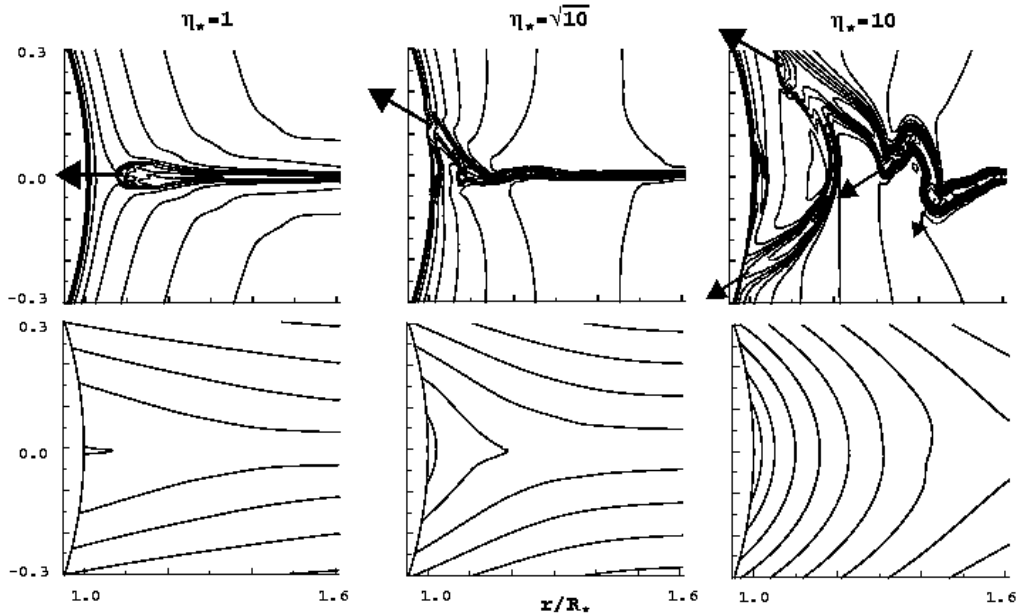


Figure 2. Contours of $\log(\text{density})$ (upper row) and magnetic field lines (lower row) for the inner, magnetic-equator regions of MHD models with moderate ($\eta_* = 1$; left), strong ($\eta_* = \sqrt{10}$; middle), and strongest ($\eta_* = 10$; left) magnetic confinement, shown at a fixed, arbitrary time snapshot well after ($t \geq 400$ ksec) the initial condition. The arrows represent the direction and magnitude of the mass flux, and show clearly that the densest structures are undergoing an infall back onto the stellar surface.